JOURNAL OF APPLIED ELECTROCHEMISTRY 6 (1976) 507–514

Electrochemical behaviour of copper in a NaF-AlF_3-$BaCl_2$ ternary melt at 750° C

J. CHRYSSOULAKIS, J. DE LEPINAY, M. J. BARBIER

E.N.S. d'electrochimie et d'electrometallurgie, B.P. 44, Domaine Universitaire, 38401 – Saint Martin d'Heres – France

Received 20 November 1975

Voltammetric and chronopotentiometric methods were used to study the electrochemical behaviour of copper in the NaF–AlF_3–$BaCl_2$ ternary melt at 750° C. Copper, graphite and platinum were used as electrode materials. It was shown that the electrochemical reduction of copper ions is a single step process, with the reversible exchange of one electron at a copper electrode. The value of the diffusion coefficient of the cuprous ion, determined by means of chronopotentiometry, is $D = (2{\cdot}8 \pm 0{\cdot}3) \times 10^{-5}\,cm^2\,s^{-1}$.

1. Introduction

There have been a few reports concerning the electrochemistry of copper in molten fluoride media [1–7].

For a NaF–KF melt at 850° C, Grjotheim established [2] an electromotive force series in which the Cu (I)/Cu couple is placed at + 0·48 V relative to the Ni (II)/Ni couple.

Studying various molten chloride media, Delimarskii [5] found the degree of oxidation to be 1 for copper ions in the temperature range 500–700° C. He also studied [7] by means of polarography the electrochemical reduction of CuO dissolved in the Na_3AlF_6–NaF eutectic at 1000° C.

None of these studies provides any data directly applicable for electrolytic aluminum metal refining purposes. In this case, the electrolyte used is a melt having the following weight composition:

NaF	17%
AlF_3	23%
$BaCl_2$	60%.

We began, therefore, our work with the investigation of the electrochemical properties of pure copper in this melt. The measurements were performed using triangular voltammetry and then made more precise by means of chronopotentiometry.

2. Operating conditions

2.1. *Solutions*

The solvent was a mixture of NaF (Pro Anal), AlF_3 (bisublimate supplied by Pechiney Soc.) and $BaCl_2$. We used $BaCl_2 \cdot 2H_2O$ (Prolabo RP) dehydrated by heating at 450° C under an argon atmosphere; this salt was then ground and preheated at 450° C before use.

The solute used was CuCl (Pro Anal) containing $CuCl_2$ traces which we eliminated by washing with 36 N H_2SO_4, followed by repeated rinsings with ethyl alcohol and diethyl oxide and finally drying at 150° C.

2.2. *Electrodes*

The working electrodes used (ET) were (Fig. 1) graphite (ϕ = 1 mm) and platinum rods (ϕ = 0·5 mm) whose surface areas could be changed according to the technique proposed by Canoo and Claes [8].

The fine adjustment of the immersion depth was made possible by means of a micrometric screw (precision 1/100 mm) permitting variations of the electrode area of a known value. This differential procedure allowed an improved measurement of area assuming the cancelling of the error due to the electrolyte meniscus appear-

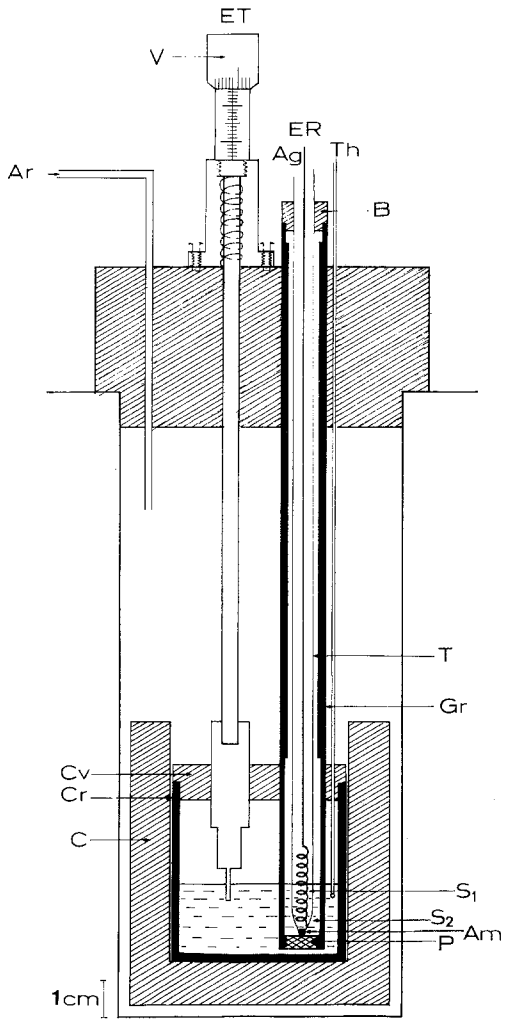

Fig. 1. Cross-section of the experimental cell.

ing at the surface level of the bath. Moreover, it allowed us to check the reproducibility of each increment of the electrode area.

However, as far as the chronopotentiometric measurements were concerned, we also used copper and graphite plates with a geometrical area between 1 and 1·5 cm^2 as working electrodes.

The auxiliary electrode was a vitreous carbon plate (Carbone Lorraine V 10) with an approximate area of 4 cm^2. It was immersed vertically.

The reference electrode (ER) was $Ag^+(M)/Ag$ similar to that suggested by Coriou [9], i.e. a silver wire (Ag) immersed in a molar solution of AgCl in NaCl–KCl(S_1) molten eutectic; the whole system was inserted in a quartz tube (T). The electrolyte junction was achieved by means of a capillary orifice filled with an asbestos cork (Am). This set was maintained inside a graphite tube (Gr) (Vicarb TFA), containing the NaCl–KCl eutectic pure melt (S_2) by means of a steatite stopper (B). A graphite pill (P) screwed at the bottom of this tube provides the electrolyte junction with the melt.

2.3. *Experimental cell*

The electrolyte was contained in a vitreous carbon crucible (Cr) ($\phi = 4{\cdot}6$ cm) (Carbone Lorraine V 10) placed at the bottom of a steatite box (C); the cover of the crucible (Cv) was perforated to allow the insertion of the electrodes.

2.4. *Electrical circuit*

The current was supplied to the electrolytic cell by means of a potentiostat (Tacussel PRT 20–2X) monitored by a signal generator (Tacussel-GSATP). The voltammetric curves were recorded by means of a differential storage oscilloscope (Tektronix 564 B) equipped with two differential amplifiers (2A–63) which permitted the X–Y recording. The current variations were deduced from the voltage drop through a resistance connected in series with the auxiliary electrode. The chronopotentiometric device was described by Poignet [10].

3. Limiting electrode processes of the solvent

In order to distinguish between electrochemical reactions concerning copper and those concerning the solvent, we have established i–(e) curves using triangular voltammetry applied to a graphite electrode in the pure solvent. We observed (Fig. 2):

(a) A cathodic peak A with an amplitude of $-1{\cdot}9$ A cm^{-2} at $e = -1{\cdot}4$ V/Ag^+(M)/Ag, corresponding to the reduction of the aluminium ions; we verified that this peak did not appear in an AlF_3 free NaF–$BaCl_2$ melt. We obtained no evidence for Al_4C_3 formation on the electrode surface. The value of the reduction potential of aluminum on graphite ($-1{\cdot}060$ V/Ag^+(M)/Ag), obtained by extrapolation (Fig. 2), is in good agreement with that measured for the equilibrium potential of liquid aluminum ($-1{\cdot}050$ V/Ag^+(M)/Ag).

(b) At potentials more negative than $e = -2$ V/Ag^+

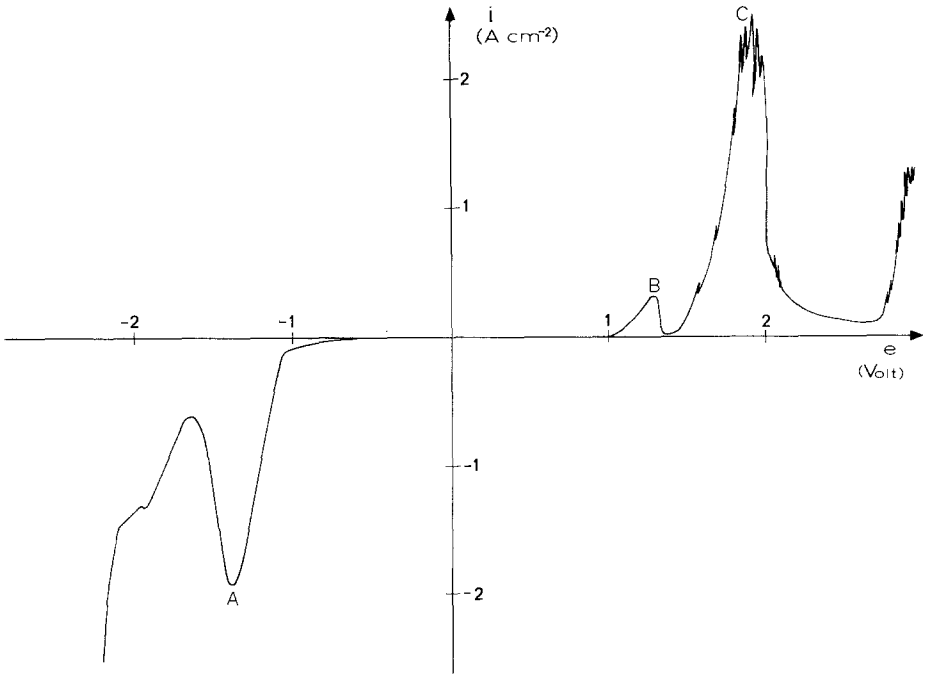

Fig. 2. Current–potential curve showing the potential span between the limiting electrode reactions (graphite electrode). Sweep rate: $v = 1\ \mathrm{V\ min^{-1}}$.

(M)/Ag, current density increased because of the reduction of Ba^{2+} ions [11–14].

In the anodic potential range, we observed:

(a) The oxidation (B) of the remaining oxide ions to oxygen at $e = 1\ \mathrm{V/Ag^+(M)/Ag}$. This was confirmed by the increase of the peak current density when we added small quantities of Al_2O_3 (0 to $6{\cdot}1 \times 10^{-5}\ \mathrm{mol\ cm^{-3}}$).

(b) Chlorine evolution (C) at $e = 1{\cdot}5\ \mathrm{V/Ag^+(M)/Ag}$ followed by a current decrease due to a gas accumulation upon the electrode area [15].

(c) The oxidation of fluoride ions [11, 14] at a potential varying from $2{\cdot}7\ \mathrm{V/Ag^+(M)/Ag}$ to $4\ \mathrm{V/Ag^+(M)/Ag}$ for a sweep rate of $1\ \mathrm{V\ s^{-1}}$.

4. Study of copper behaviour

4.1. *Voltammetric study*

We obtained a cathodic peak at the potential $e_p = -0{\cdot}55 \pm 0{\cdot}03\ \mathrm{V/Ag^+(M)/Ag}$ using a graphite electrode and $e_p = -0{\cdot}5 \pm 0{\cdot}02\ \mathrm{V/Ag^+(M)/Ag}$ when a platinum electrode was used for a sweep rate $v = 1\ \mathrm{V\ s^{-1}}$ and a Cu(I) concentration $C^0 = 10{\cdot}8 \times 10^{-5}\ \mathrm{mol\ cm^{-3}}$ CuCl.

Fig. 3 (a and b) presents voltammograms performed respectively with a graphite electrode ($\phi = 1$ mm) and a platinum electrode ($\phi = 0{\cdot}5$ mm) for a sweep rate $v = 1\ \mathrm{V\ s^{-1}}$. Between two successive curves, a 1 mm variation was applied to the immersion depth of the electrode.

The shape of this peak Fig. 3(a) and the existence of a sharp anodic stripping peak (Fig. 4) were typical of an insoluble deposit [16] when a graphite electrode was used, whereas we observed that the activity of the deposit was time-dependent when a platinum electrode was used (Fig. 3b).

Fig. 3(a) clearly demonstrates that the ohmic drop effect on voltammetric transients is not at all negligible. Unfortunately, we could not extrapolate the values of the peak potential to $I_p = 0$ at a fixed sweep speed as the ohmic impedance of the electrodes assembly did not remain constant when the immersion depth increased. If we consider a 1 mm diameter graphite electrode for instance, the resistance decreased from between 3 and 4 Ω for a 2 mm immersion depth to approximately 2 Ω when the depth reached 8 mm.

The initial slope of the voltammograms at the start of the peak (Fig. 4) at a graphite electrode, where all transients are identical when the current begins to increase significantly, is also character-

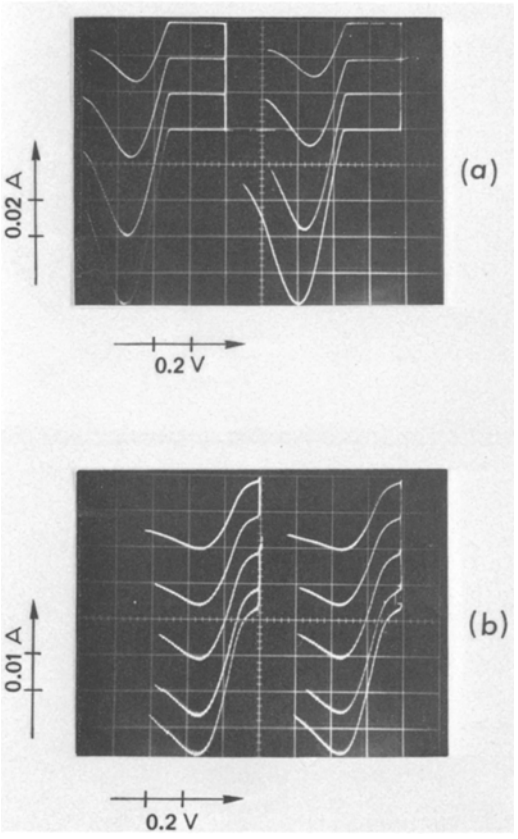

Fig. 3. Series of voltammetric curves I (e/Ag$^+$(M)/Ag) obtained for a graphite $\phi = 1$ mm (a) and a platinum $\phi = 0{\cdot}5$ mm (b) electrode for increasing immersion depths (right) and decreasing immersion depths (left). For clarity, the origins of the different curves have been shifted vertically. $C^0 = 42{\cdot}5 \times 10^{-5}$ mol cm^{-3} CuCl; initial immersion depth: 2 mm; sweep rate: 1 V s^{-1}.

istic of an important ohmic drop limitation. The variations of the peak and half-peak potentials versus the current intensity when the sweep speed was changed are straight lines parallel to the linear variation $e(I)$ recorded at the beginning of the cathodic peak. The d.d.p. between the initial line and the peak line on the one hand, and the half-peak line on the other hand, were $0{\cdot}070 \pm 0{\cdot}015$ V and $0{\cdot}060 \pm 0{\cdot}012$ V respectively. These differences remained almost constant for sweep speeds up to about 5 V s^{-1} and increased slightly for higher speeds; this behaviour corresponds to some possible quasi-irreversibility of the electrochemical reaction or to an incomplete coverage of the electrode area by the diffusion layers with respect to the too short time elapsed, before the theoretical peak potential. We made similar observations concerning the cathodic deposit of copper on platinum rods ($\phi = 0{\cdot}5$ mm) for which the distance between the peak and half-peak lines was found to be approximately 0·12 V.

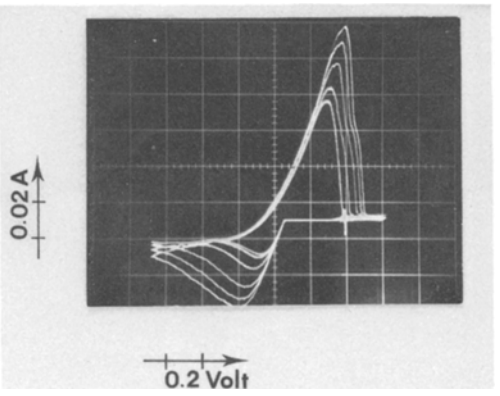

Fig. 4. Current–potential triangular voltammetric transients for a graphite electrode in a $42{\cdot}5 \times 10^{-5}$ mol cm^{-3} CuCl solution at the following sweep rates: $v = 0{\cdot}5;1;2;3;4$ V s^{-1}; geometrical surface area: 7·1 mm^2.

Assuming that the displacements of the peak and half-peak potentials with the sweep speed arise essentially from the ohmic drop, Fig. 5 shows that e_p in both cases (curve 1: graphite; curve 2: platinum) and the $e_{p/2} - e_p$ difference (curve 3: graphite; curve 4: platinum) increases linearly versus the square root of the sweep rate. The extrapolations of these straight lines to $v = 0$ yielded:

$(e_{p/2} - e_p)_0 = 0{\cdot}06$ V for the graphite electrode;

$(e_{p/2} - e_p)_0 = 0{\cdot}12$ V for the platinum electrode;

and

$(e_p - e_{initial})_0 = -0{\cdot}081$ V for the graphite electrode.

The corresponding theoretical values [16] for the reversible exchange of one electron and the formation of an insoluble deposit at 750° C are respectively:

$e_{p/2} - e_p = 0{\cdot}068$ V; $e_p - e_{initial} = -0{\cdot}0752$ V.

When the product is soluble, $e_{p/2} - e_p = 0{\cdot}194$ V [16]. This comparison of the theoretical and experimental values precludes the possibility that more than a single electron is involved in the electrochemical reaction.

In order to determine the diffusion coefficient of the Cu(I) species, we studied the peak current

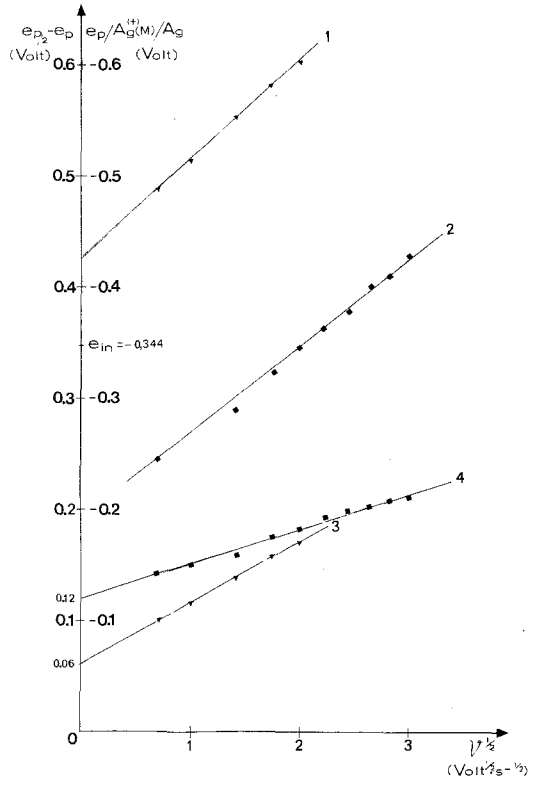

Fig. 5. Plot of $e_p/Ag^+(M)/Ag$ and $e_{p/2} - e_p$ versus the square root of the sweep rate $v^{1/2}$ at graphite (curves 1 and 3) and platinum (curves 2 and 4) electrodes. $C^0 = 42{\cdot}5 \times 10^{-5}$ mol cm^{-3} CuCl.

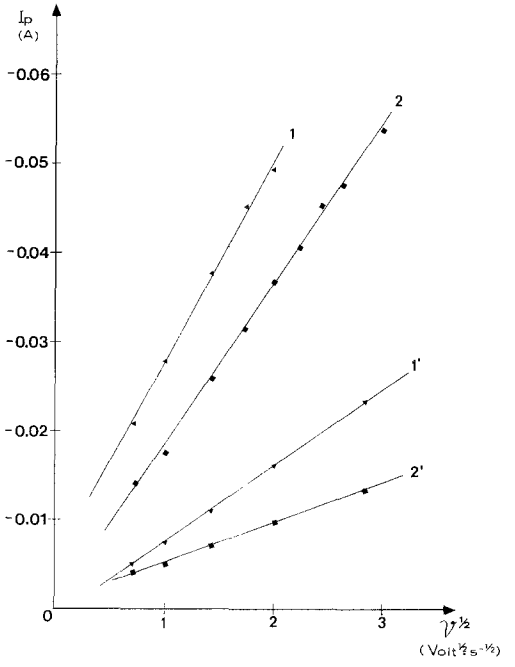

Fig. 6. Plot of the peak current i_p versus the square root of sweep rate $v^{1/2}$.
Curve 1 (graphite electrode) $C^0 = 42{\cdot}5 \times 10^{-5}$ mol cm^{-3} CuCl. Curve 1′ (graphite electrode) $C^0 = 10{\cdot}8 \times 10^{-5}$ mol cm^{-3} CuCl; Curve 2 (platinum electrode) $C^0 = 42{\cdot}5 \times 10^{-5}$ mol cm^{-3} CuCl; Curve 2′ (platinum electrode) $C^0 = 10{\cdot}8 \times 10^{-5}$ mol cm^{-3} CuCl.

density Δi_p dependency both on the CuCl concentration and on the electrode immersion depth.

Table 1 shows the mean value of the ratio of the peak current density variation to the concentration $\Delta i_p/C^0$ for ten consecutive depth increments in solutions in the concentration range $5{\cdot}4 \times 10^{-5}$–1×10^{-3} mol cm^{-3} of CuCl.

We observed that $\Delta i_p/C^0$ is not concentration dependent, but that it is less reproducible with graphite than with the platinum electrodes. We even noted that $\Delta i_p/C^0$ tends to increase with C^0 at graphite electrodes whereas it would be expected to drift in the opposite direction owing to the drop in the actual sweep rate resulting from the increasing participation of the ohmic drop. This behaviour may be explained by the growth of more large dendrites when the concentration (and, consequently, the current density) was increased.

Moreover, i_p is a linear function of $v^{1/2}$ (Fig. 6) for both graphite (curve 1 and 1′) and platinum (curves 2 and 2′) electrodes. The diffusion coef-

Table 1. Average values of $\Delta i_p/C^0$ *for different* CuCl *concentrations with graphite and platinum electrodes. Sweep rate:* $V = 1$ V s^{-1}

C^0 (mol cm^{-3} CuCl)	*Graphite* $\Delta i_p/C^0$ (A mol^{-1} cm)	*Platinum* $\Delta i_p/C^0$ (A mol^{-1} cm)
$5{\cdot}45 \times 10^{-5}$	$(1{\cdot}25 \pm 0{\cdot}7) \times 10^3$	$(1{\cdot}1 \pm 0{\cdot}4) \times 10^3$
$10{\cdot}8 \times 10^{-5}$	$(1{\cdot}17 \pm 0{\cdot}3) \times 10^3$	$(1{\cdot}05 \pm 0{\cdot}1) \times 10^3$
$21{\cdot}42 \times 10^{-2}$	$(1{\cdot}24 \pm 0{\cdot}2) \times 10^3$	$(0{\cdot}94 \pm 0{\cdot}05) \times 10^3$
$42{\cdot}5 \times 10^{-5}$	$(1{\cdot}65 \pm 0{\cdot}1) \times 10^3$	$(0{\cdot}88 \pm 0{\cdot}05) \times 10^3$
$84{\cdot}75 \times 10^{-5}$		$(0{\cdot}9 \pm 0{\cdot}06) \times 10^3$

ficient of the copper ions in the electrolyte at 750° C can, therefore, be calculated [16].

We obtained, with a graphite electrode, $D = (4{\cdot}7 \pm 2) \times 10^{-5}$ cm^2 s^{-1} (the cathodic deposit is insoluble). With a platinum electrode, we found $D = (2{\cdot}5 \pm 0{\cdot}7) \times 10^{-5}$ cm^2 s^{-1} assuming an insoluble deposit and $D = (4{\cdot}5 \pm 1{\cdot}3) \times 10^{-5}$ cm^2 s^{-1} assuming a soluble product. Variations and lack of reproducibility of the active surface areas of the electrodes especially as far as the graphite electrodes are concerned, and the magnitude of the ohmic drop precluded a detailed analysis of the voltammetric results.

In order to avoid the difficulties arising from the ohmic drop interference and the questionable nature of the deposit on the platinum electrode, we carried on this study by means of chronopotentiometry. With respect to the active surface area reproducibility, better results will be expected for the diffusion coefficient determination from measurements performed with platinum electrodes.

4.2. *Chronopotentiometric study*

We observed a single transition time with graphite, copper and platinum electrodes. The transition times were measured according to the Reinmuth procedure [17].

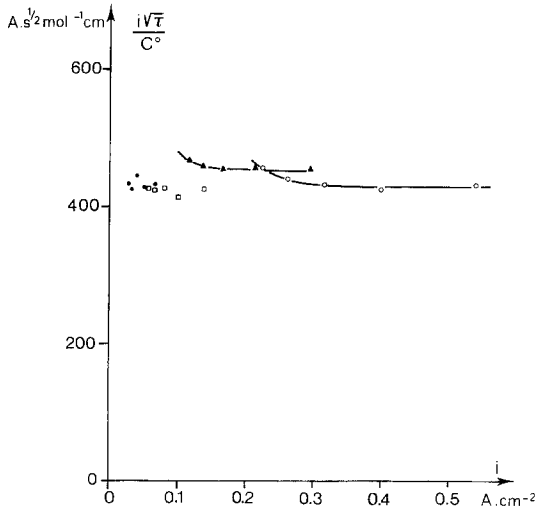

Fig. 7. Plot of $i\tau^{1/2}/C^0$ against i for platinum electrodes. • $C^0 = 5{\cdot}03 \times 10^{-5}$ mol cm^{-3} CuCl; □ $C^0 = 9{\cdot}9 \times 10^{-5}$ mol cm^{-3} CuCl; ▲ $C^0 = 20{\cdot}1 \times 10^{-5}$ mol cm^{-3} CuCl; ○ $C^0 = 39{\cdot}8 \times 10^{-5}$ mol cm^{-3} CuCl.

A set of $i\tau^{1/2}/C^0$ against i plots, achieved with a transition time range 0·1–0·8 s is reported in Fig. 7, showing that the Sand's equation is obeyed under these experimental conditions. Nevertheless, $i\tau^{1/2}/C^0$ began to shift up to higher values when the chronopotentiogram duration exceeded 0·5 s (i.e. for the smallest current densities). Such a behaviour is more typical of natural convection than any surface effect, as significant positive drifts of $i\tau^{1/2}/C^0$, corresponding to successive surface area enlargements arising from the larger currents involved, did not result from each concentration increase.

Typical potential–time curves recorded at a copper electrode for different current densities are shown in Fig. 8. The initial potential steps observed at the starts of the chronopotentiograms are the ohmic drops remaining unchanged along each transient. The overpotential, $e_{\tau/4}$, at a quarter of the transition time, did not depend on current density. The experimental value $e_{\tau/4} = -0{\cdot}051 \pm 0{\cdot}002$ V is comparable with the theoretical value: $-0{\cdot}061$ V for the reversible one-electron process [16].

The $e = f[\log(\sqrt{\tau} - \sqrt{t})/\sqrt{\tau}]$ plots obtained with a copper electrode (curve 1), a graphite electrode (curve 2) and a platinum electrode (curve 3) are shown in Fig. 9. The potential

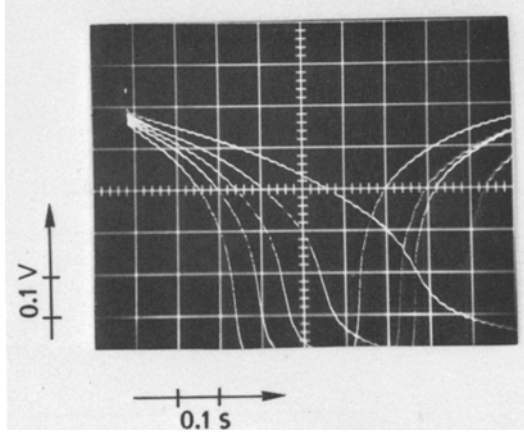

Fig. 8. Chronopotentiograms for a copper electrode for the following current densities:
$i = 0{\cdot}1, 0{\cdot}12, 0{\cdot}13, 0{\cdot}146, 0{\cdot}166$ A cm^{-2}; $C^0 = 8 \times 10^{-5}$ mol cm^{-3} CuCl
N.B. Using copper electrode with much larger surface areas (1–1·5 cm^2) than the graphite and platinum ones (0·04–0·25 cm^2) with a different shape, the resistance of the cell assembly was about 0·3 Ω instead of the 2–4 Ω previously encountered.

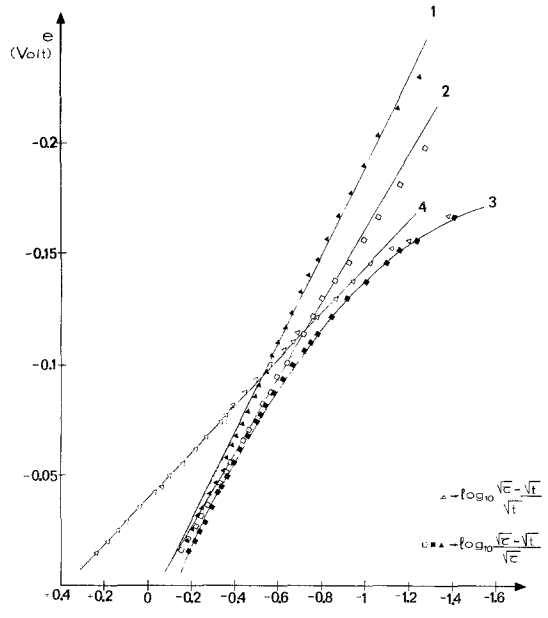

Fig. 9. Chronopotentiometric electrode solubility test for the cathodic reduction of cuprous ions.
Curve 1: copper electrode ($C^0 = 12 \times 10^{-5}$ mol cm^{-3});
Curve 2: graphite electrode ($C^0 = 15{\cdot}6 \times 10^{-5}$ mol cm^{-3});
Curves 3 and 4: platinum electrode ($C^0 = 9{\cdot}9 \times 10^{-5}$ mol cm^{-3}).

variations are linear in the case of copper and graphite electrodes, showing that the cathodic product is insoluble. The electron number, computed from the slopes of the plots, amounted to $n = 1{\cdot}02$ for the copper electrode (slope = 0·20 V dec^{-1}) and $n = 1{\cdot}2$ for the graphite electrode (slope = 0·17 V dec^{-1}).

When platinum electrodes were used, the electrode potential e varied linearly versus log $(\sqrt{\tau} - \sqrt{t}/\sqrt{t})$ (Fig. 9, plot 4) whereas the plot versus $\log(\sqrt{\tau} - \sqrt{t}/\sqrt{\tau})$ (Fig. 9, plot 3) was curved, thus confirming the results of the voltammetric investigation.

Table 2 presents $[\Delta(\sqrt{\tau_{x+1}} - \sqrt{\tau_x})i]/C^0$ values obtained for four 1 mm immersion depth increments and four different concentrations:
x is the immersion depth in mm;
$i = I/\Delta S$ is the ratio of the current intensity to the area increment;
Thus, $[\Delta(\sqrt{\tau_{x+1}} - \sqrt{\tau_x})i]/C^0 = (nF\sqrt{n}\sqrt{D})/2$.
whence $D = (2{\cdot}8 \pm 0{\cdot}3) \times 10^{-5}$ cm^2 s^{-1}.

Table 2. Average values of $[\Delta(\sqrt{\tau_{x+1}} - \sqrt{\tau_x})i]/C^0$ *for different* CuCl *concentrations at a platinum electrode.*

C^0 (mol cm^{-3})	$[\Delta(\sqrt{(\tau_{x+1})} - \sqrt{\tau_x})i]/C^0$ (A s$^{1/2}$ mol^{-1} cm)
$5{\cdot}03 \times 10^{-5}$	$(4{\cdot}44 \pm 0{\cdot}20) \times 10^2$
$9{\cdot}9 \times 10^{-5}$	$(4{\cdot}47 \pm 0{\cdot}15) \times 10^2$
$20{\cdot}1 \times 10^{-5}$	$(4{\cdot}52 \pm 0{\cdot}2) \times 10^2$
$39{\cdot}8 \times 10^{-5}$	$(4{\cdot}64 \pm 0{\cdot}4) \times 10^2$

5. Conclusion

We have shown by means of voltammetry and chronopotentiometry that the electrochemical reduction of copper ions in the aluminium refining bath occurs according to a single step process involving the exchange of only one electron. With copper electrodes, this process, producing an insoluble deposit, was shown to be quite reversible. The transients obtained on graphite electrodes were also typical of the formation of an insoluble deposit, but were altered by significant surface area changes. At platinum electrodes, the activity of the copper deposit was not constant, leading to a rather complicated kinetic process implying underpotential effects. These results are in good agreement with the following cathodic reduction scheme:

$$Cu^+ + e^- \rightarrow Cu.$$

Having regard to the better surface area reproducibility of the electrodes the diffusion coefficient measurements were performed with platinum electrodes. Using chronopotentiometric data, we found $D = (2{\cdot}8 \pm 0{\cdot}3) \times 10^{-5}$ cm^2 s^{-1}.

References

[1] G. Grube and P. Hantelmann, *Z. Elektrochem.* **56** (1952) 1.
[2] K. Grjotheim, *Z.f. Physikal Chem. Neue Folge*, **11** (1957) 150.
[3] H. Kido, T. Rokujo and Y. Hayakawa, *J. Electrochem. Soc. Japan*, (Overseas Ed.), **27** (1957) E-12.
[4] Y. Hayakawa and Y. Imakita, *ibid* (Overseas Suppl. Ed.), **28** (1960) E-238.
[5] Iu. K. Delimarskii and B. F. Markov, 'Electrochemistry of Fused Salts', Sigma Press, Washington D.C. (1961) p. 186.
[6] S. Senderoff, *Met. Rev.*, **11** (1966) 97.
[7] Iu. K. Delimarskii and N. A. Pavlenko, *Ukrain. khim. Zhur.* **33** (1967) 130.
[8] C. Canoo and P. Claes, *Electrochim. Acta*, **19** (1974) 37.
[9] H. Coriou, J. Dirian and J. Hure, *J. Chim. phys.* **52** (1955) 479.
[10] J. C. Poignet and M. J. Barbier, *Electrochim. Acta*, 17 (1972) 1227.

[11] V. A. Garmata and A. I. Belyaev, *Tsvet. Metall.* **30** (1957) 58.
[12] L. A. Firsanova and M. I. Lavrentyev, Proc. Res. Inst. Non Ferrous Metals, (1968, Pub. 1971) 222.
[13] M. I. Lavrentyev, L. A. Firsanova and A. N. Malakhovskii, *Tsvet. Metall.* **2** (1967) 52.
[14] V. A. Garmata and A. I. Belyaev, *Sbornik Nauch. Trudov Moskov. Inst. Tsvetnykh Metall. i Zolota.* **27** (1957) 193.
[15] R. Tunold and T. Berge, *Electrochim. Acta*, **19** (1974) 849.
[16] P. Delahay, 'New Instrumental Methods in Electrochemistry', Interscience, New York (1965) p. 115.
[17] W. H. Reinnuth, *Anal. Chem.* **33** (1961) 485.